Myofibroblast activation in colorectal cancer lymph node metastases

T M Yeung*,[1,2,3], C Buskens[1,4], L M Wang[5], N J Mortensen[2,3] and W F Bodmer[1]

[1]Cancer and Immunogenetics Laboratory, Weatherall Institute of Molecular Medicine, John Radcliffe Hospital, University of Oxford, Oxford, UK; [2]Nuffield Department of Surgical Sciences, University of Oxford, Oxford, UK; [3]Department of Colorectal Surgery, University of Oxford, Oxford, UK; [4]Department of Surgery, Amsterdam Medical Center, Amsterdam, The Netherlands and [5]Department of Cellular Pathology and Oxford Biomedical Research Centre, University of Oxford, Oxford, UK

Background: Myofibroblasts have an important role in regulating the normal colorectal stem cell niche. While the activation of myofibroblasts in primary colorectal cancers has been previously described, myofibroblast activation in lymph node metastases has not been described before.

Methods: Paraffin-embedded lymph node sections from patients with macrometastases, micrometastases and isolated tumour cells were stained to identify myofibroblasts and to characterise the distribution of different cell types in tumour-containing lymph nodes. The extent of myofibroblast presence was quantified and compared with the size of the metastasis and degree of proliferation and differentiation of the cancer cells.

Results: We show substantial activation of myofibroblasts in the presence of colorectal metastases in lymph nodes, which is intimately associated with glandular structures, both in micro- and macrometastases. The degree of activation is positively associated with the size of the metastases and the proportion of Ki67 + ve cancer cells, and negatively associated with the degree of enterocyte differentiation as measured by CK20 expression.

Conclusion: The substantial activation of myofibroblasts in tumour-containing lymph nodes strongly suggests that these metastatic cancer cells are still significantly dependent on their microenvironment. Further understanding of these epithelial–mesenchymal interactions could lead to the development of new therapies in metastatic disease.

Colorectal pericryptal cells are myofibroblasts (Richman *et al*, 1987) and are presumed to have an important role in regulating the normal intestinal stem cell niche (Yen and Wright, 2006; Kosinski *et al*, 2007; Mifflin *et al*, 2011; Yeung *et al*, 2011a). They have also been shown to promote the survival of intestinal stem cells (Ootani *et al*, 2009) and colorectal cancer (CRC) stem cells (Vermeulen *et al*, 2010), and epithelial–mesenchymal interactions are critical in regulating the differentiation of CRC cells (Richman and Bodmer, 1988). An increase in the number of myofibroblasts around adenomatous colorectal polyps (Adegboyega *et al*, 2002) and primary tumour sites (Tsujino *et al*, 2007) has been previously described, and been shown to correlate with a higher rate of disease recurrence (Tsujino *et al*, 2007). However, the importance of the microenvironment in the establishment of lymph node metastases is not clear.

The presence of macrometastases in the lymph node (> 2 mm in diameter) is clinically significant as it is associated with a poorer prognosis (O'Connell *et al*, 2004). However, there is still a major question as to the clinical importance of isolated tumour cells (ITCs) (< 0.2 mm) and micrometastases (0.2–2 mm) (Hata *et al*, 2011; Rahbari *et al*, 2012) in lymph nodes of patients with CRC. Up to 25% of patients with Dukes B stage of CRC die with tumour recurrence and this may be owing to occult disease. Multiple levels of lymph nodes are not routinely examined histologically, and small metastatic deposits may easily be missed, with the patient consequently being understaged (Greenson *et al*, 1994; Rosenberg *et al*, 2002; Hata *et al*, 2011).

In this study, we show that myofibroblasts are substantially activated when colorectal metastases develop within lymph nodes. This strongly suggests that the metastatic tumour cells attempt to

recreate the microenvironment observed in primary tumours and, indeed, in the normal stem cell niche. This is in marked contrast to the normal lymph node, where myofibroblasts are found only around the capsule and not within the body of the lymph node. The myofibroblasts are very closely associated with glandular structures, recapitulating the close relationship found between pericryptal myofibroblasts and normal colonic columnar epithelial cells. Myofibroblasts are present in micrometastases, although to a lesser extent than in macrometastases, supporting the notion that micrometastases are viable and interacting with the microenvironment, thus demonstrating their probable clinical significance.

MATERIALS AND METHODS

Archived paraffin-embedded lymph nodes obtained from patients undergoing surgery for CRC were identified retrospectively through searching pathology reports for the key terms 'isolated tumour cells', 'micrometastases' and 'macrometastases'. Material was obtained from two centres (Oxford University Hospitals, UK and Amsterdam Medical Centre, The Netherlands) and approved by the local research ethics committee. Serial sections with H&E were obtained from the Oxford specimens and examined by a
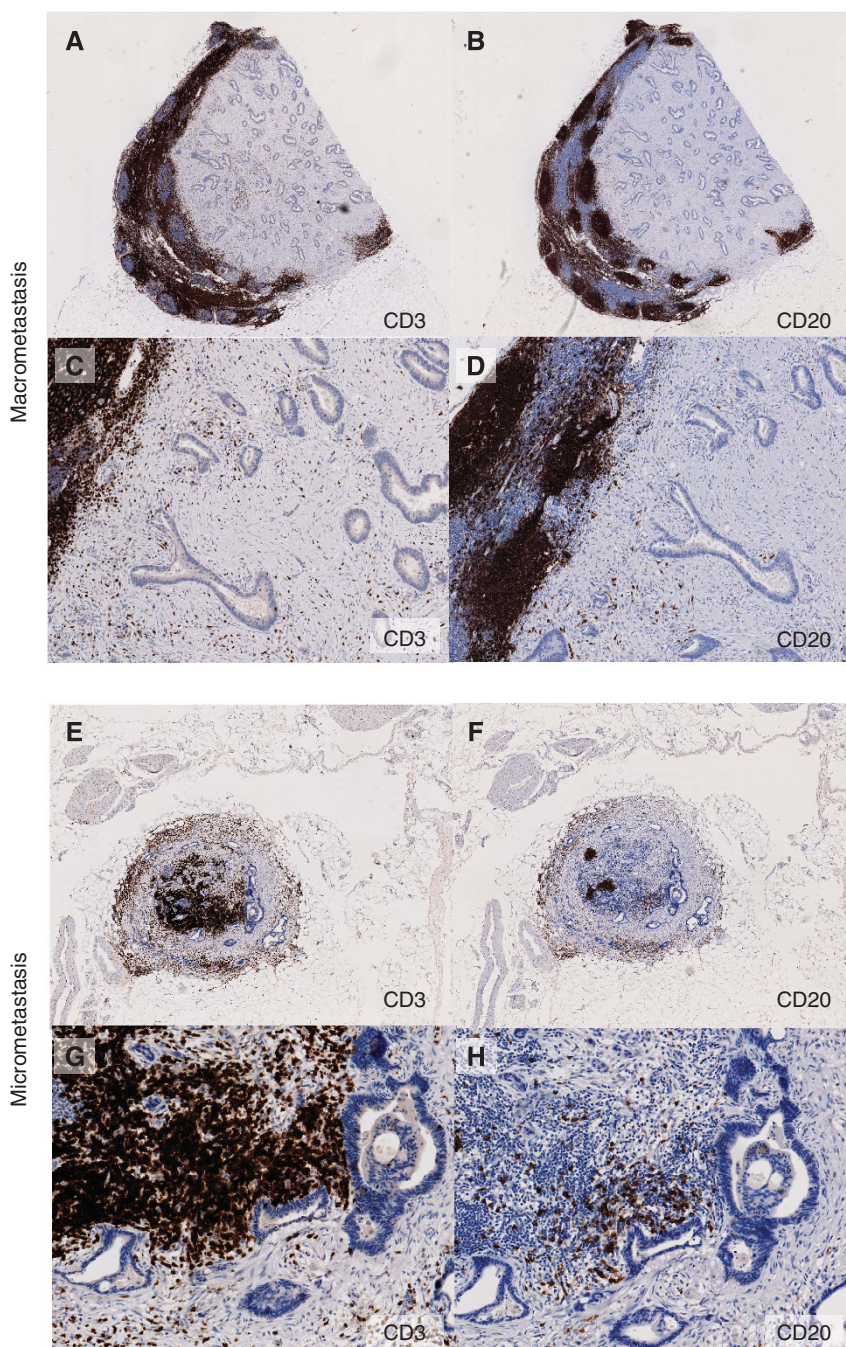

Figure 1. Metastatic CRC in lymph nodes has a high proportion of stromal tissue as compared with glandular structures. Colorectal adenocarcinoma macrometastasis expanding to fill almost the entire lymph node, stained with (A) CD3 for T-lymphocytes and (B) CD20 for B-lymphocytes. × 1 magnification. (C) CD3 and (D) CD20 × 10 magnification. Most of the metastasis is filled with stromal tissue as compared with glandular structures. Colorectal adenocarcinoma micrometastasis filling the periphery of the lymph node, with the remaining lymphocytes in the center (E) CD3 and (F) CD20 × 2 magnification. (G) and (H) × 10 magnification.

consultant histopathologist (LMW) to confirm the presence and location of ITCs, micrometastases and macrometastases.

Immunohistochemistry and immunofluorescence were performed according to standard protocols. Paraffin-embedded sections were deparaffinised in xylene twice for 3 min, and hydrated in 100% ethanol, 100% industrial methylated spirit (IMS) and 70% IMS for 2 min each. Slides were rinsed in distilled water. Antigen retrieval was performed using Target Retrieval solution (Dako, Ely, UK, pH 6.1 at 100 °C for 20 min) followed by cooling to room temperature for 1 h. Slides were blocked at room temperature for 30 min using Invitrogen blocking reagent (0.1 g 10 ml^{-1} in PBS-Tween 0.05%, Invitrogen, Life Technologies, Paisley, UK). Slides were next incubated at room temperature for 1 h with the appropriate primary antibody in blocking solution.

These antibodies included α-smooth muscle actin-FITC (αSMA, clone 1A4, Sigma Aldrich, Gillingham, Dorset, UK, 1:200), AUA-1 anti-EpCAM mAb (in-house, 1:200), CAM5.2 mAb (in-house, 1:200), CK20 mAb (Dako, 1:100), Ki67 mAb (clone MIB1, Dako, 1:100), Vimentin mAb (clone 3B4, Dako, 1:100), Desmin mAb (clone D33, Dako, 1:100), CD31 mAb (in-house, 1:20, Oxford University Hospitals, Department of Cellular Pathology), CD34 mAb (Dako, 1:25), CD3 mAb (Dako 1:50), CD20 mAb (Dako 1:200), CD45 (Dako Clone 2B11+PD7/26, 1:100) and human HGF (R&D, Abingdon, UK, 1:40).

The secondary antibody used was HRP-conjugated goat anti-mouse (Invitrogen, 1:100) or Zymax rabbit anti-goat HRP (Invitrogen, 1:200), and was revealed by immunofluorescence (Tyramide AlexaFluor, Invitrogen) or immunohistochemistry
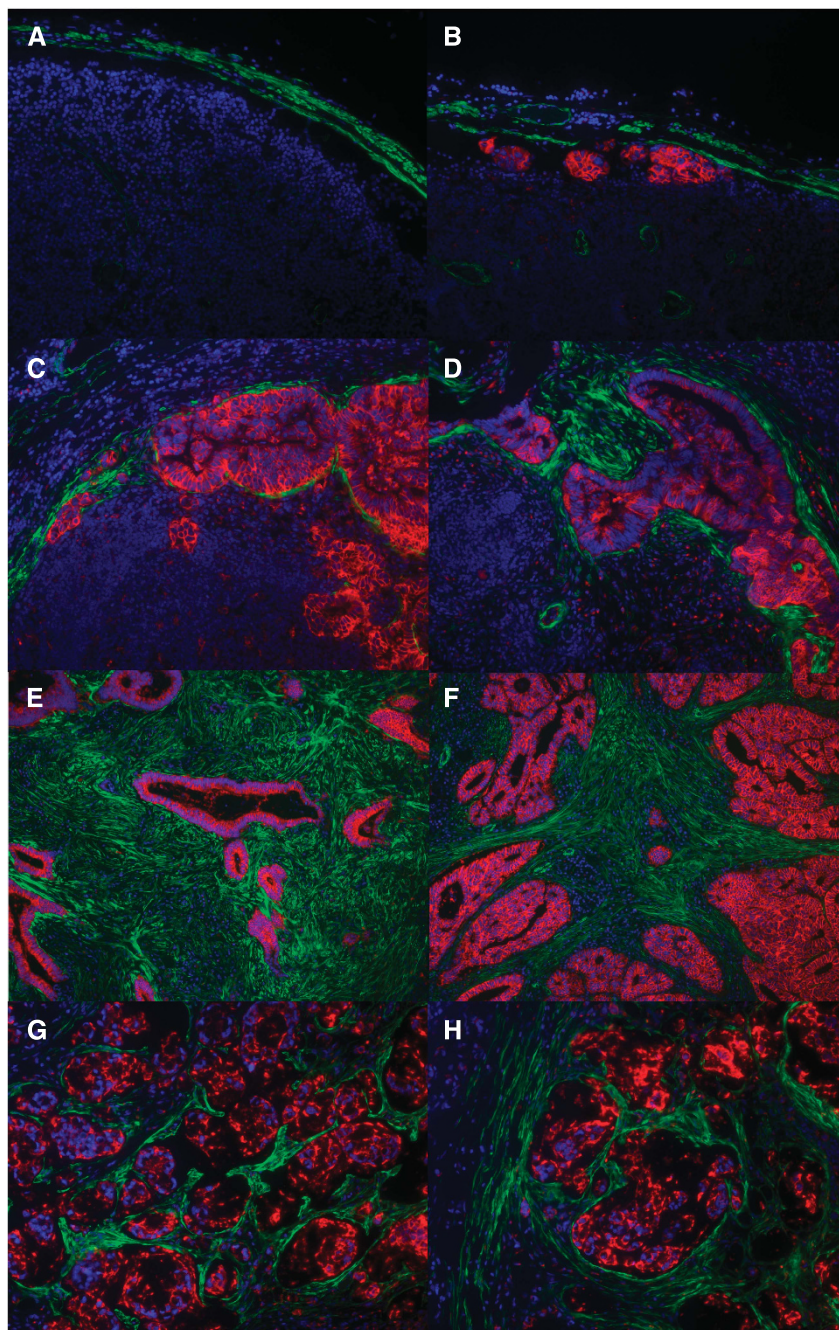

Figure 2. Myofibroblasts are intimately associated with CRC lymph node metastases. Costaining of paraffin-embedded sections of lymph nodes with αSMA (green) for myofibroblasts and AUA-1 (red) to identify epithelial cells. (A) Normal lymph node ×20 magnification. (B) Isolated tumour cells ×20 magnification.(C) and (D) Micrometastasis ×20 magnification. (E) and (F) Macrometastasis ×10 magnification. (G) and (H) Macrometastasis with signet ring cell morphology ×20 magnification. All from different patients apart from (G) and (H).

(DAB). Images were obtained using a Zeiss Axioscope 2 Plus microscope or a Zeiss LSM confocal microscope (Zeiss, Cambridge, UK).

Quantification of immunofluorescence. All images were viewed and analysed using ImageJ software (NIH, Bethesda, MD, USA). To measure the proportion of lymph node metastasis that was positive for myofibroblasts, the area of fluorescent myofibroblasts was circumscribed and measured, then divided by the area of the lymph node metastasis, as defined by the area containing epithelial glands and stromal tissue.

To measure the fluorescence of αSMA and CK20, the total and background fluorescence for each lymph node metastasis were calculated, and the background fluorescence was subtracted from the total before being used for statistical analysis, as previously described (Yeung *et al*, 2011b).

To quantify Ki67 + cells, the number of Ki67 + cells in each gland was counted, and divided by the total number of cells in the gland.

RESULTS

Metastatic CRC in lymph nodes has a high proportion of stromal tissue as compared with glandular structures. Analysis of H&E-stained metastatic lymph nodes suggested that much of the abnormal tissue was stromal, rather than just glandular epithelium. Staining consecutive sections with CD3 (T-lymphocytes) (Alibaud *et al*, 2000) and CD20 (B-lymphocytes) (Mason *et al*, 1990) showed that there was comparatively little infiltration by lymphocytes into the cancer-associated stromal tissue (Figure 1C and D), and that the advancing metastasis distorted the normal follicular architecture of lymph nodes. (Figure 1A and B). We also observed that there was limited infiltration of CD45-positive cells (also known as common leucocyte antigen) in the stroma (Supplementary Figure S1). A similar picture was seen in micrometastases, where there was also extensive stromal tissue surrounding the cancer cells (Figure 1E–H).

Myofibroblasts are intimately associated with CRC lymph node metastases and make up the bulk of the stromal tissue in involved lymph nodes. Given the close association of myofibroblasts with both normal colonic crypts and primary CRC, involved and uninvolved lymph nodes were costained with αSMA (green) to identify myofibroblasts and AUA-1 (in-house antibody against EpCAM, red) (Spurr *et al*, 1986) to identify epithelial cells (Figure 2, further examples shown in Supplementary Figure S2). In the normal lymph node, αSMA expression was overwhelmingly limited to the exterior capsule, showing that myofibroblasts were limited to the exterior capsule area and were not seen within the body of the lymph node (Figure 2A). The identification of ITCs in the subcapsular region of lymph nodes (Figure 2B) is consistent with the anatomy of draining lymph, which first enters the lymph node in the subcapsular space. In micrometastases, myofibroblasts are found intimately surrounding glandular structures in the same way that they surround the normal colonic crypt (Figure 2C and D). In macrometastases, there is widespread expansion and infiltration of myofibroblasts (Figure 2E and F), corresponding to the observations in Figure 1 of an excess of stromal as compared with glandular tissue within intra-lymph node tumour masses. Recruitment of myofibroblasts can also be seen in tumour metastases with signet ring cell morphology (Figure 2G and H), although in this case there are no glandular structures and there appears to be a lower proportion of myofibroblasts to tumour cells than in macrometastases of the usual type.

As myofibroblasts have been shown to maintain the stem-like phenotype of CRC stem cells through the production of HGF (Vermeulen *et al*, 2010), we also ascertained whether HGF was also present in the myofibroblast microenvironment surrounding lymph node metastases (Figure 3). We observed that HGF was closely associated with AUA-1-positive CRC metastases, situated adjacent to myofibroblasts, which strongly suggests that HGF also has an important role in maintaining the stem-like phenotype of CRC stem cells in the metastatic niche.

To confirm that these αSMA-positive cells were myofibroblasts, we stained for vimentin (for fibroblasts) and desmin (for smooth muscle). The cancer-associated stromal cells were αSMA positive, vimentin positive (Figure 4B) and desmin negative (Figure 4G–I), confirming their identity as myofibroblasts (Mifflin *et al*, 2011). For comparison, normal lymph nodes do express high levels of vimentin, but this staining does not colocalise with αSMA; these
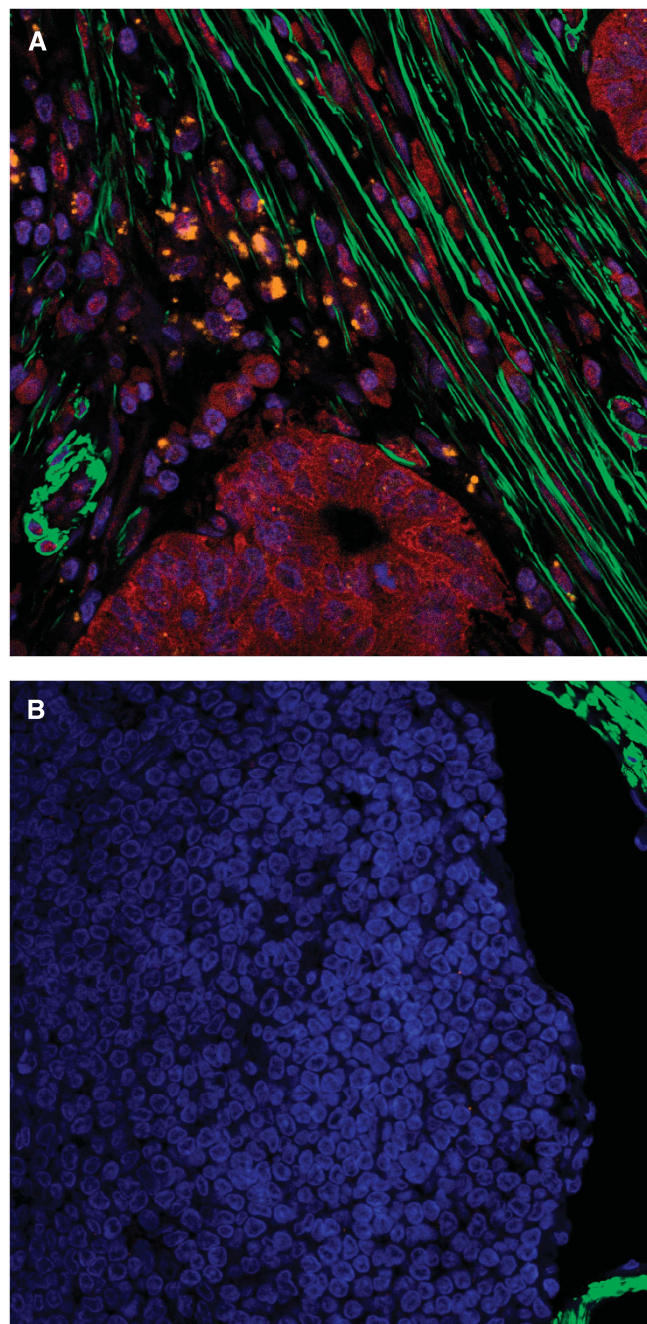

Figure 3. Presence of HGF in the metastatic lymph node microenvironment. Confocal immunohistochemistry of (**A**) macrometasis and (**B**) normal lymph node tissue. αSMA (green), AUA-1 (red), HGF (orange), × 40 magnification.

vimentin-positive cells represent the reticulum or endothelial cells (Figure 4A) (Giorno, 1985). Similarly, desmin is only expressed in areas containing smooth muscle and does not colocalise with αSMA-positive myofibroblasts in the involved lymph node (Figure 4G). We also examined whether vascular structures could be contributing to the bulk of the stromal tissue. Staining for CD31 (Parums *et al*, 1990) and CD34 (Ramani *et al*, 1990), markers of vascular endothelium in the normal lymph node (Figure 4C and E), demonstrated that only a small proportion of the stromal tissue contained these vascular structures in the involved lymph node (Figure 4D and F).

The degree of myofibroblast involvement increases with the size of the metastasis. To investigate the relationship between myofibroblast involvement and size of metastasis, we examined patient lymph nodes with single cells, ITCs, micrometastases and macrometastases. Epithelial cells were identified by Cam5.2 (Makin *et al*, 1984), a monoclonal antibody that is predominately against CK8, and reacts strongly with all colorectal adenocarcinoma epithelial cells. Quantification of the degree of αSMA for each size of metastasis reveals a significant increase of myofibroblast involvement with increasing size of metastasis, most strikingly with the macrometastases (Figure 5).

The degree of myofibroblast involvement is positively correlated with Ki67 staining for cell division, and inversely correlated with CK20 staining, a marker of enterocyte differentiation. Involved lymph nodes were stained with Ki67 to assess the incidence of dividing cells. Metastatic areas containing a high proportion of Ki67 + CRC cells were associated with significantly higher levels of
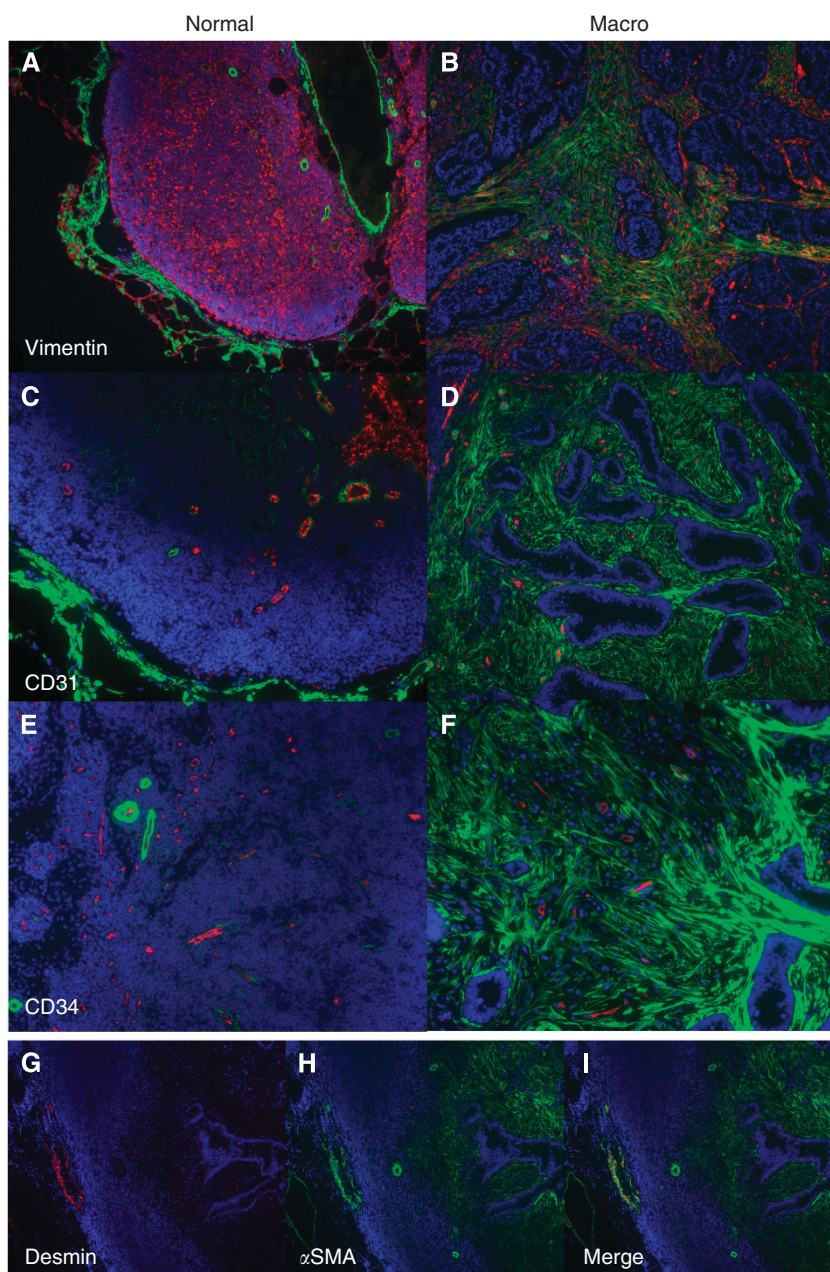

Figure 4. Characterisation of stromal tissue within normal lymph nodes (**A,C,E**) and macrometastases (**B, D, F–I**). Costaining of paraffin-embedded sections of lymph nodes with αSMA (green) and (**A**), (**B**) vimentin (red) × 10 magnification, (**C**), (**D**) CD31(red) × 20 magnification, (**E**), (**F**) CD34 (red) × 20 magnification. Staining of macrometastasis: (**G**) Desmin (red), (**H**) αSMA (green) and (**I**) Merge × 10 magnification.

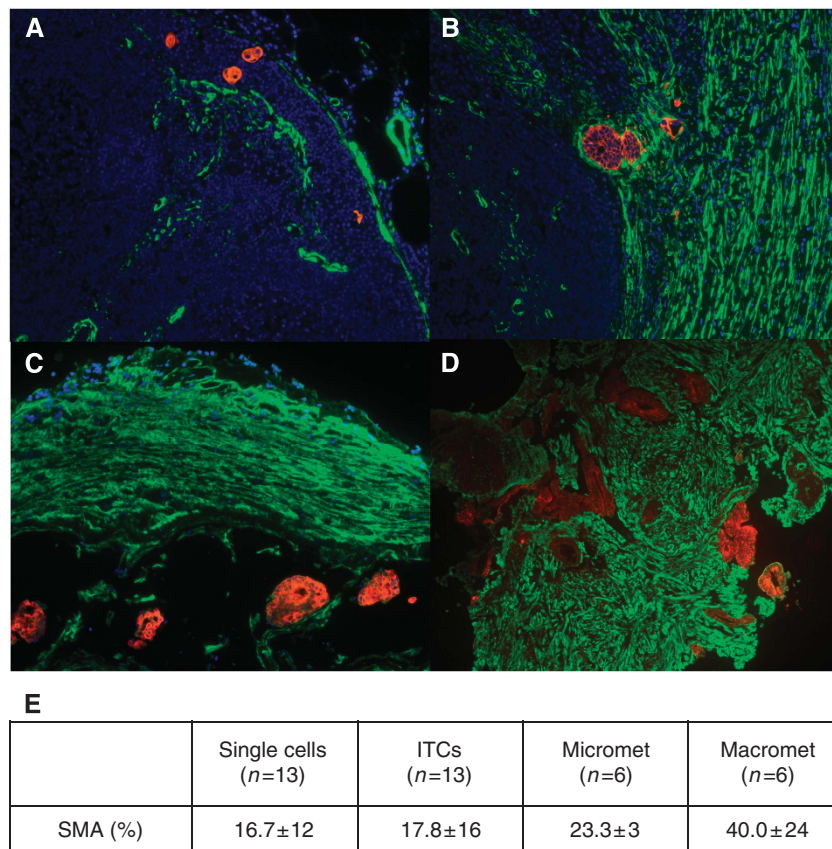| E	Single cells (n=13)	ITCs (n=13)	Micromet (n=6)	Macromet (n=6)
SMA (%)	16.7±12	17.8±16	23.3±3	40.0±24

Figure 5. Correlation between extent of αSMA staining and size of metastasis. Costaining using Cam5.2 (Red) and αSMA (Green) of lymph nodes with (A) single epithelial cells ×20 magnification, (B) isolated tumour cells (ITCs) ×20 magnification, (C) micrometastasis ×20 magnification and (D) macrometastasis ×10 magnification. (E) Quantification of area of αSMA staining for each metastatic group. Total of 38 lymph nodes all from different patients. Values represent mean ± s.d.

myofibroblasts (Figure 6A–C), compared with areas with a low proportion of Ki67+ epithelial cells (Figure 6D and E), and quantitative analysis showed that this difference was highly statistically significant (Figure 6F). Conversely, when involved lymph nodes were stained with CK20 as a marker of enterocyte differentiation, there was an inverse relationship between the extent of myofibroblast involvement and the level of CK20 staining (Figure 7A–G). This association was also highly statistically significant when quantified (Figure 7H).

DISCUSSION

We have shown that myofibroblasts, as identified by αSMA and vimentin costaining, occur abundantly within lymph nodes containing CRC metastases. This is in complete contrast to normal uninvolved lymph nodes where no internal myofibroblasts are seen. It thus appears most probable that the CRC metastases are activating the myofibroblasts, leading to their recruitment into the lymph node. Although a desmoplastic reaction is often described in histological reports in relation to the primary tumour (Gregoire and Lieubeau, 1995; Ueno et al, 2004; Hirose et al, 2010), the degree of myofibroblast activation in metastatic lymph nodes has not been described before. Our results imply that the assumption that aggressive cancers become independent of their microenvironment when establishing distant metastases needs to be reconsidered. Understanding the relationship between myofibroblasts and lymph node metastases is not just of prognostic significance (Tsujino et al, 2007); it could provide a new

therapeutic target for the treatment of cancer, even in advanced stages.

Small isolated CA cell deposits preferentially appear just under the lymph node capsule, where cancer cells would first enter the lymph node via the subcapsular space. The normal capsule contains myofibroblasts, and therefore provides an anchorage point for metastasising cells to establish themselves when they first enter the lymph node. Consistent with this is the finding that micrometastases are also found adjacent to the capsule; some micrometastases appear to grow within the capsule, being completely surrounded by the myofibroblasts within the capsule. This suggests that the capsule is a source of the activated myofibroblasts seen in lymph node metastases. Other sources, such as the bone marrow, however, may also contribute to the mass of activated myofibroblasts (Brittan et al, 2002; Direkze et al, 2004). Fibrocytes are reported to be bone marrow-derived mesenchymal progenitor cells that express CD45 and CD34, and have the ability to differentiate into myofibroblasts, resulting in the loss of expression of CD45/CD34 and an increase in expression of αSMA (Bellini and Mattoli, 2007; Grieb et al, 2011). The vast majority of cells in the stroma surrounding colorectal metastases are not CD45+ (Supplementary Figure S1) nor CD34+ (Figure 4), suggesting that most of these cells are of the myofibroblast phenotype. A recent study suggested that 20% of tumour-associated myofibroblasts originated from bone marrow and mesenchymal stem cells (Quante et al, 2011), possibly from fibrocytes. However, that would leave the remaining 80% still most probably coming from local sources, including in particular the capsule of the lymph node.
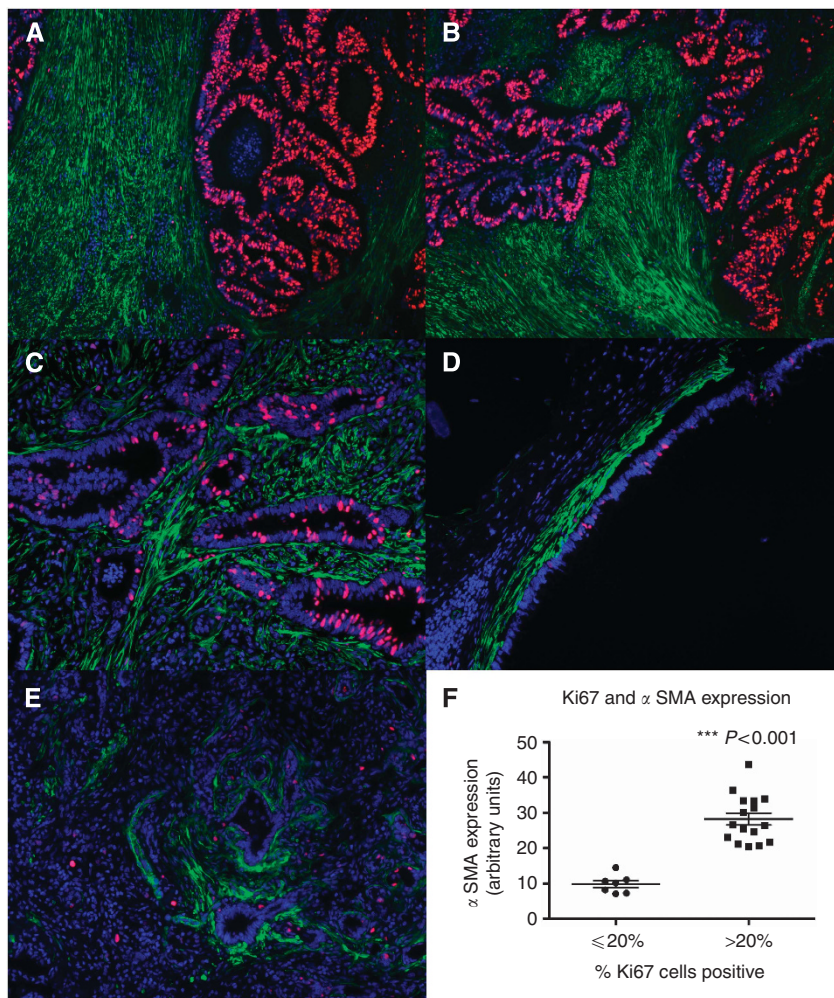
Figure 6. Extent of myofibroblast involvement is positively associated with the proportion of dividing epithelial cells as measured by Ki67 staining. Paraffin-embedded sections of macrometastases were costained with αSMA (green) and with Ki67(for dividing cells) (red). (**A**), (**B**) High proportion of Ki67 + cells × 10 magnification. (**C**) High proportion of Ki67 + cells × 20 magnification. (**D**) and (**E**) Low proportion of Ki67 + cells × 20 magnification. (**F**) Quantification of proportion of Ki67 + cells in relation to level of αSMA fluorescence. Data showed bimodality at 20% (Supplementary Figure S3A), therefore the cutoff was chosen to be this point.

The myofibroblast activation does not appear to be just a passive reaction to the metastatic invasions of lymph nodes. The fact that cancer cells attach specifically to the capsule when they enter the lymph node strongly supports a role for capsular myofibroblasts in helping these metastatic cells establish themselves by providing a supportive microenvironment. Myofibroblast activation is seen in both primary tumours and hepatic metastases (Tsujino *et al*, 2007; Matsusue *et al*, 2009), suggesting that this involves a bidirectional interaction in which epithelial cells secrete products, most probably growth factors or cytokines, that stimulate myofibroblasts that, in turn, release similar but different factors that promote the growth and invasion of the cancer epithelial cells. In this way, the cancer is able to create significant aspects of the microenvironment found in the primary tumour, and indeed of the normal stem cell niche.

We did observe that the level of Ki67 expression in myofibroblasts was low. This may be owing to myofibroblasts having proliferated extensively initially and once they have reached a certain mass threshold, they return to a lower level of proliferation. Alternatively, it could be a reflection of the fact that the expression of Ki67 in background lymphoid cells and cancerous epithelial cells is very high; therefore any expression of Ki67 in myofibroblasts would be relatively low in comparison with these two types of cells.

The clinical significance of micrometastases in CRC and whether pathologists should routinely perform multiple level section examination on all lymph nodes retrieved remain controversial. The fact that micrometastases are also inducing myofibroblast activation strongly suggests that even at an early stage, micrometastases are viable, interact with their microenvironment, have the potential to continue growing and are therefore clinically important.

This adds further weight to the view that each lymph node should be examined thoroughly to exclude the presence of micrometastases, as missing them could result in understaging and undertreating patients (Hata *et al*, 2011). This is further supported by a recent systematic review and meta-analysis that showed that the molecular detection of tumour cells in lymph nodes is associated with disease recurrence and poorer survival in patients defined initially as being node-negative on conventional histopathological analysis, as compared with patients in whom molecular analysis did not detect any cancer cells (Rahbari *et al*, 2012).

Myofibroblasts support the growth and repair of mouse and human intestinal epithelium both *in vitro* and *in vivo* (Ootani *et al*, 2009; Lahar *et al*, 2011; Normand *et al*, 2011) through a complex interaction of Wnt, BMP and Hedgehog pathways (Yeung *et al*,
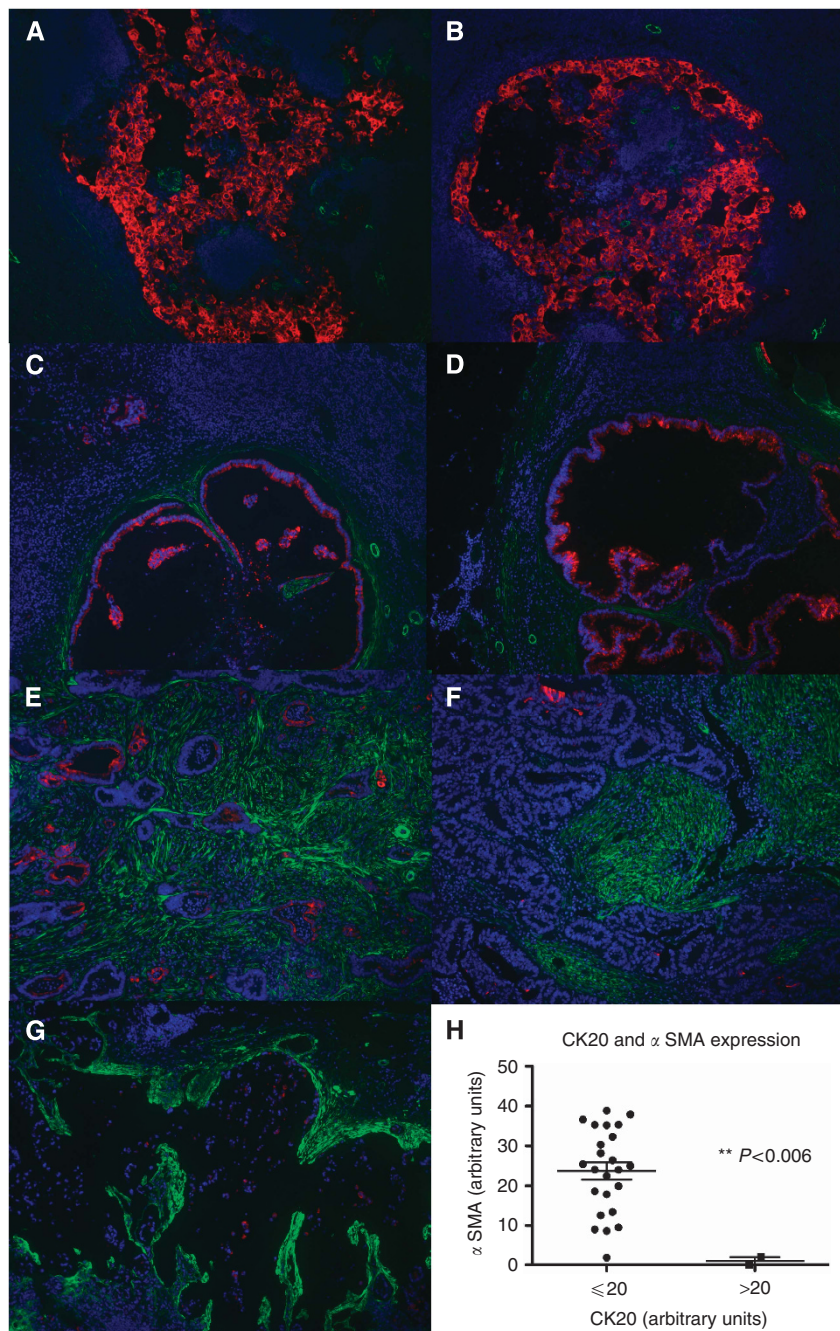
Figure 7. Extent of myofibroblast involvement is inversely associated with the level of CK20 expression. Paraffin-embedded sections of macrometastases were costained with αSMA (green) together with CK20 (a measure of enterocyte differentiation) (red). (A), (B) High CK20 expression × 10 magnification. (C), (D) Moderate CK20 expression × 10 magnification. (E), (F) Low CK20 expression × 10 magnification. (G) Tumour metastasis with signet ring cell morphology and scanty CK20 expression × 10 magnification. (H) Quantification of expression of CK20 in relation to level of αSMA fluorescence. Data showed bimodality at 20 (Supplementary Figure S3B), therefore the cutoff was chosen to be this point.

2011a). Myofibroblasts have also been shown to maintain the stem-like phenotype of CRC stem cells through the secretion of HGF (Vermeulen et al, 2010). Consistent with this is our finding that tumour glands with a stem-like phenotype (Yeung et al, 2010), containing a higher proportion of Ki67 + ve cells and a lower expression of CK20, are associated with a higher degree of myofibroblast activation. We observed that HGF was present in the myofibroblast microenvironment surrounding lymph node metastases, which suggests that HGF also has an important role in maintaining CRC stem cells in the metastatic niche.

Histologically, we see an organised arrangement of myofibroblasts closely surrounding glandular structures in well-differentiated tumours, recapitulating the arrangement of myofibroblasts in a normal stem cell niche. In contrast, we observed that cancerous glands that contain a higher proportion of cells with a stem-like phenotype are associated with more myofibroblast activation and arranged in a disorganised manner. This is consistent with a previous study by Ueno et al (2004) who looked at primary rectal cancers, and showed that myofibroblasts were distributed more extensively in immature fibrotic stroma

compared with mature and intermediate fibrotic stroma, and this was associated with a poorer survival.

CONCLUSIONS

The presence of activated myofibroblasts in lymph nodes containing metastatic colorectal adenocarcinoma highlights the importance of the microenvironment in supporting cancers, even in late metastatic stages. Further understanding of the interaction between myofibroblasts and metastases may provide novel therapeutic targets for late-stage as well as early-stage disease.

ACKNOWLEDGEMENTS

REFERENCES

Adegboyega PA, Mifflin RC, DiMari JF, Saada JI, Powell DW (2002) Immunohistochemical study of myofibroblasts in normal colonic mucosa, hyperplastic polyps, and adenomatous colorectal polyps. *Arch Pathol Lab Med* **126**(7): 829–836.

Alibaud L, Llobera R, Al Saati T, March M, Delsol G, Rubin B (2000) A new monoclonal anti-CD3epsilon antibody reactive on paraffin sections. *J Histochem Cytochem* **48**(12): 1609–1616.

Bellini A, Mattoli S (2007) The role of the fibrocyte, a bone marrow-derived mesenchymal progenitor, in reactive and reparative fibroses. *Lab Invest* **87**(9): 858–870.

Brittan M, Hunt T, Jeffery R, Poulsom R, Forbes SJ, Hodivala-Dilke K, Goldman J, Alison MR, Wright NA (2002) Bone marrow derivation of pericryptal myofibroblasts in the mouse and human small intestine and colon. *Gut* **50**(6): 752–757.

Direkze NC, Hodivala-Dilke K, Jeffery R, Hunt T, Poulsom R, Oukrif D, Alison MR, Wright NA (2004) Bone marrow contribution to tumor-associated myofibroblasts and fibroblasts. *Cancer Res* **64**(23): 8492–8495.

Giorno R (1985) Immunohistochemical analysis of the distribution of vimentin in human peripheral lymphoid tissues. *Anat Rec* **211**(1): 43–47.

Greenson JK, Isenhart CE, Rice R, Mojzisik C, Houchens D, Martin Jr EW (1994) Identification of occult micrometastases in pericolic lymph nodes of Duke's B colorectal cancer patients using monoclonal antibodies against cytokeratin and CC49. Correlation with long-term survival. *Cancer* **73**(3): 563–569.

Gregoire M, Lieubeau B (1995) The role of fibroblasts in tumor behavior. *Cancer Metastasis Rev* **14**(4): 339–350.

Grieb G, Steffens G, Pallua N, Bernhagen J, Bucala R (2011) Circulating fibrocytes–biology and mechanisms in wound healing and scar formation. *Int Rev Cell Mol Biol* **291**: 1–19.

Hata M, Machi J, Mamou J, Yanagihara ET, Saegusa-Beecroft E, Kobayashi GK, Wong CC, Fung C, Feleppa EJ, Sakamoto K (2011) Entire-volume serial histological examination for detection of micrometastases in lymph nodes of colorectal cancers. *Pathol Oncol Res* **17**(4): 835–841.

Hirose M, Fukui H, Igarashi Y, Fujimori Y, Katake Y, Sekikawa A, Ichikawa K, Tomita S, Imura J, Ajioka Y, Ueno H, Hase K, Ohkura Y, Kashida H, Togashi K, Nishigami T, Matsui T, Yao T, Wada R, Matsuda K, Watanabe D, Ochiai A, Sugai T, Sugihara K, Fujimori T (2010) Detection of desmoplastic reaction in biopsy specimens is useful for predicting the depth of invasion of early colorectal cancer: a Japanese collaborative study. *J Gastroenterol* **45**(12): 1212–1218.

Kosinski C, Li VS, Chan AS, Zhang J, Ho C, Tsui WY, Chan TL, Mifflin RC, Powell DW, Yuen ST, Leung SY, Chen X (2007) Gene expression patterns of human colon tops and basal crypts and BMP antagonists as intestinal stem cell niche factors. *Proc Natl Acad Sci USA* **104**(39): 15418–15423.

Lahar N, Lei NY, Wang J, Jabaji Z, Tung SC, Joshi V, Lewis M, Stelzner M, Martin MG, Dunn JC (2011) Intestinal subepithelial myofibroblasts support *in vitro* and *in vivo* growth of human small intestinal epithelium. *PLoS One* **6**(11): e26898.

Makin CA, Bobrow LG, Bodmer WF (1984) Monoclonal antibody to cytokeratin for use in routine histopathology. *J Clin Pathol* **37**(9): 975–983.

Mason DY, Comans-Bitter WM, Cordell JL, Verhoeven MA, van Dongen JJ (1990) Antibody L26 recognizes an intracellular epitope on the B-cell-associated CD20 antigen. *Am J Pathol* **136**(6): 1215–1222.

Matsusue R, Kubo H, Hisamori S, Okoshi K, Takagi H, Hida K, Nakano K, Itami A, Kawada K, Nagayama S, Sakai Y (2009) Hepatic stellate cells promote liver metastasis of colon cancer cells by the action of SDF-1/CXCR4 axis. *Ann Surg Oncol* **16**(9): 2645–2653.

Mifflin RC, Pinchuk IV, Saada JI, Powell DW (2011) Intestinal myofibroblasts: targets for stem cell therapy. *Am J Physiol Gastrointest Liver Physiol* **300**(5): G684–G696.

Normand S, Delanoye-Crespin A, Bressenot A, Huot L, Grandjean T, Peyrin-Biroulet L, Lemoine Y, Hot D, Chamaillard M (2011) Nod-like receptor pyrin domain-containing protein 6 (NLRP6) controls epithelial self-renewal and colorectal carcinogenesis upon injury. *Proc Natl Acad Sci USA* **108**(23): 9601–9606.

O'Connell JB, Maggard MA, Ko CY (2004) Colon cancer survival rates with the new American Joint Committee on Cancer sixth edition staging. *J Natl Cancer Inst* **96**(19): 1420–1425.

Ootani A, Li X, Sangiorgi E, Ho QT, Ueno H, Toda S, Sugihara H, Fujimoto K, Weissman IL, Capecchi MR, Kuo CJ (2009) Sustained *in vitro* intestinal epithelial culture within a Wnt-dependent stem cell niche. *Nat Med* **15**(6): 701–706.

Parums DV, Cordell JL, Micklem K, Heryet AR, Gatter KC, Mason DY (1990) JC70: a new monoclonal antibody that detects vascular endothelium associated antigen on routinely processed tissue sections. *J Clin Pathol* **43**(9): 752–757.

Quante M, Tu SP, Tomita H, Gonda T, Wang SS, Takashi S, Baik GH, Shibata W, Diprete B, Betz KS, Friedman R, Varro A, Tycko B, Wang TC (2011) Bone marrow-derived myofibroblasts contribute to the mesenchymal stem cell niche and promote tumor growth. *Cancer Cell* **19**(2): 257–272.

Rahbari NN, Bork U, Motschall E, Thorlund K, Buchler MW, Koch M, Weitz J (2012) Molecular detection of tumor cells in regional lymph nodes is associated with disease recurrence and poor survival in node-negative colorectal cancer: a systematic review and meta-analysis. *J Clin Oncol* **30**(1): 60–70.

Ramani P, Bradley NJ, Fletcher CD (1990) QBEND/10, a new monoclonal antibody to endothelium: assessment of its diagnostic utility in paraffin sections. *Histopathology* **17**(3): 237–242.

Richman PI, Bodmer WF (1988) Control of differentiation in human colorectal carcinoma cell lines: epithelial-mesenchymal interactions. *J Pathol* **156**(3): 197–211.

Richman PI, Tilly R, Jass JR, Bodmer WF (1987) Colonic pericrypt sheath cells: characterisation of cell type with new monoclonal antibody. *J Clin Pathol* **40**(6): 593–600.

Rosenberg R, Hoos A, Mueller J, Baier P, Stricker D, Werner MNekarda H, Siewert JR (2002) Prognostic significance of cytokeratin-20 reverse transcriptase polymerase chain reaction in lymph nodes of node-negative colorectal cancer patients. *J Clin Oncol* **20**(4): 1049–1055.

Spurr NK, Durbin H, Sheer D, Parkar M, Bobrow L, Bodmer WF (1986) Characterization and chromosomal assignment of a human cell surface antigen defined by the monoclonal antibody AUAI. *Int J Cancer* **38**(5): 631–636.

Tsujino T, Seshimo I, Yamamoto H, Ngan CY, Ezumi K, Takemasa I, Ikeda M, Sekimoto M, Matsuura N, Monden M (2007) Stromal myofibroblasts predict disease recurrence for colorectal cancer. *Clin Cancer Res* **13**(7): 2082–2090.

Ueno H, Jones AM, Wilkinson KH, Jass JR, Talbot IC (2004) Histological categorisation of fibrotic cancer stroma in advanced rectal cancer. *Gut* **53**(4): 581–586.

Vermeulen L, De Sousa EMF, van der Heijden M, Cameron K, de Jong JH, Borovski T, Tuynman JB, Todaro M, Merz C, Rodermond H, Sprick MR, Kemper K, Richel DJ, Stassi G, Medema JP (2010) Wnt activity defines

colon cancer stem cells and is regulated by the microenvironment. *Nat Cell Biol* **12**(5): 468–476.

Yen TH, Wright NA (2006) The gastrointestinal tract stem cell niche. *Stem cell Rev* **2**(3): 203–212.

Yeung TM, Chia LA, Kosinski CM, Kuo CJ (2011a) Regulation of self-renewal and differentiation by the intestinal stem cell niche. *Cell Mol Life Sci* **68**(15): 2513–2523.

Yeung TM, Gandhi SC, Bodmer WF (2011b) Hypoxia and lineage specification of cell line-derived colorectal cancer stem cells. *Proc Natl Acad Sci USA* **108**(11): 4382–4387.

Yeung TM, Gandhi SC, Wilding JL, Muschel R, Bodmer WF (2010) Cancer stem cells from colorectal cancer-derived cell lines. *Proc Natl Acad Sci USA* **107**(8): 3722–3727.

Supplementary Information accompanies this paper on British Journal of Cancer website (http://www.nature.com/bjc)